Effect of significant data loss on identifying electric signals that precede rupture estimated by detrended fluctuation analysis in natural time

E. S. Skordas, N. V. Sarlis, and P. A. Varotsos[a)]
Department of Physics, Solid State Section and Solid Earth Physics Institute, University of Athens, Panepistimiopolis, Zografos, Athens 15784, Greece

(Received 6 March 2010; accepted 23 July 2010; published online 18 August 2010)

Electric field variations that appear before rupture have been recently studied by employing the detrended fluctuation analysis (DFA) to quantify their long-range temporal correlations. These studies revealed that seismic electric signal (SES) activities exhibit a scale invariant feature with an exponent $\alpha_{\mathrm{DFA}} \approx 1$ over all scales investigated (around five orders of magnitude). Here, we study what happens upon significant data loss, which is a question of primary practical importance, and show that the DFA applied to the natural time representation of the remaining data still reveals for SES activities an exponent close to 1.0, which markedly exceeds the exponent found in artificial (man-made) noises. This enables the identification of a SES activity with probability of 75% even after a significant (70%) data loss. The probability increases to 90% or larger for 50% data loss.
 [doi:10.1063/1.3479402]

Complex systems usually exhibit scale-invariant features characterized by long-range power-law correlations, which are often difficult to quantify due to various types of nonstationarities observed in the signals emitted. This also happens when monitoring geoelectric field changes aiming at detecting seismic electric signal (SES) activities that appear before major earthquakes. To overcome this difficulty the novel method of detrended fluctuation analysis (DFA) has been employed, which when combined with a newly introduced time domain termed natural time, allows a reliable distinction of true SES activities from artificial (man-made) noises. This is so because the SES activities are characterized by "infinitely" ranged temporal correlations (resulting in DFA exponents close to unity) while the artificial noises are not (since all the noises studied to date have DFA exponents at most around 0.8). The analysis of SES observations often meets the difficulty of significant data loss caused either by failure of the data collection system or by removal of seriously noise-contaminated data segments. Here we focus on the effect of significant data loss on the long-range correlated SES activities quantified by DFA. We find that the remaining data, even after a considerable percentage of data loss (which may reach ~80%), may still be revealing the scaling properties of SES activities. This is achieved by applying DFA *not* to the original time-series of the remaining data but to those resulted when employing natural time.

I. INTRODUCTION

The output signals of complex systems exhibit fluctuations over multiple scales[1,2] which are characterized by the absence of dynamic scale, i.e., scale-invariant behavior.[3] These signals, due to the nonlinear mechanisms controlling the underlying interactions, are also typically nonstationary and their reliable analysis cannot be achieved by traditional methods, e.g., power-spectrum and autocorrelation analysis.[4–6] On the other hand, the detrended fluctuation analysis (DFA) (Refs. 7 and 8) has been established as a robust method suitable for detecting long-range power-law correlations embedded in nonstationary signals. This is so because a power-spectrum calculation assumes that the signal is stationary and hence when applied to nonstationary time-series it can lead to misleading results. Thus, a power-spectrum analysis should be necessarily preceded by a test for the stationarity of the (portions of the) data analyzed. As for the DFA, it can determine the (mono) fractal scaling properties (see below) even in nonstationary time-series, and can avoid, in principle, spurious detection of correlations that are artifacts of nonstationarities. DFA has been applied with successful results to diverse fields where scale-invariant behavior emerges, such as DNA,[9–16] heart dynamics,[17–27] circadian rhythms,[28–31] meteorology[32] and climate temperature fluctuations,[33–37] economics,[38–44] as well as in the low-frequency (≤ 1 Hz) variations of the electric field of the earth that precede earthquakes[45–47] termed seismic electric signals[48–54] and in the relevant[55–58] magnetic field variations.[47]

Monofractal signals are homogeneous in the sense that they have the same scaling properties, characterized locally by a single singularity exponent h_0, throughout the signal. Thus, monofractal signals can be indexed by a single global exponent, e.g., the Hurst exponent $H \equiv h_0$, which suggests that they are stationary from the viewpoint of their local scaling properties (see Refs. 22 and 59 and references therein). Since DFA can measure only one exponent, this method is more suitable for the investigation of monofractal signals. In some cases, however, the records cannot be accounted for by a single scaling exponent (i.e., do not exhibit a simple monofractal behavior). In general, if a multitude of

a)Electronic mail: pvaro@otenet.gr.

scaling exponents is required for a full description of the scaling behavior, a multifractal analysis must be applied. Multifractal signals are intrinsically more complex, and inhomogeneous, than monofractals (see Ref. 22 and references therein). A reliable multifractal analysis can be performed by the multifractal detrended fluctuation analysis (MF-DFA) (Refs. 60 and 61) or by the wavelet transform (e.g., see Refs. 59 and 62).

DFA has been applied, as mentioned, to the SES activities. It was found[45] that when DFA is applied to the original time-series of the SES activities and artificial (man-made) noises, both types of signals lead to a slope at short times (i.e., $\Delta t \leq 30$ s) lying in the range $\alpha = 1.1-1.4$, while for longer times the range $\alpha = 0.8-1.0$ was determined without, however, any safe classification between SES activities and artificial noises. On the other hand, when employing natural time (see Sec. II), DFA enables the distinction between SES activities and artificial noises: for the SES activities the α-values lie approximately in the range of 0.9–1.0 (or between 0.85 and 1.1, if a reasonable experimental error is envisaged), while for the artificial noises (due to man-made sources) the α-values are markedly smaller, i.e., $\alpha = 0.65-0.8$. In addition, MF-DFA has been used[45,46] and it was found that this multifractal analysis, when carried out in the conventional time frame, did not lead to any distinction between these two types of signals, but does so, if the analysis is made in the natural time domain.

The aforementioned findings of DFA for SES activities are consistent with their generation mechanism[63,64] which could be summarized as follows. Beyond the usual intrinsic lattice defects[65–70] in ionic solids in particular, because of ubiquitous aliovalent impurities, extrinsic defects are formed for charge compensation. A portion of these defects is attracted by the nearby impurities, thus forming electric dipoles the orientation of which can change by defect migration. In the focal area of an impending earthquake the stress gradually increases and hence affects the thermodynamic parameters of this migration, thus it may result in a gradual decrease of their relaxation time. When the stress (pressure) reaches a *critical* value, a *cooperative* orientation of these dipoles occurs, which leads to the emission of a transient signal. This signal constitutes the SES activity and, since it is characterized by critical dynamics, should exhibit infinitely range temporal correlations (in the sense that, as mentioned above, for SES activities $\alpha_{\mathrm{DFA}} \approx 1$ over five orders of magnitude[47]). In practice, for physical reasons, e.g., finite size effects, there is no infinity[71] but the scaling is observed over a limited range of scales and this is why we write hereafter "infinite."

It is the basic aim of this study to investigate how significant data loss affects the scaling behavior of long-range correlated SES activities. This has been inspired from a similar recent study of Ma *et al.*[72] where they also investigated the effects of data loss on long-term correlations and introduced a new segmentation approach to generate surrogate signals by randomly removing data segments from stationary signals with different types of long-range correlations. The practical importance of this study becomes very clear upon considering that such a data loss is inevitable mainly due to the following two reasons. First, failure of the measuring system in the field station, including the electric measuring dipoles, electronics, and the data collection system, may occur especially due to lightning. Second, noise-contaminated data segments are often unavoidable due to natural changes such as rainfall, lightning, induction of geomagnetic field variations, and ocean-earth tides besides the noise from artificial (man-made) sources including the leakage currents from dc driven trains. The latter are common in Japan where at some sites high man-made noise may last for almost 70% of the time every day. We clarify, however, that even at such noisy-stations in Japan, several clear SES activities have been unambiguously identified[73] during the night (when the noise level is low). In addition, prominent SES activities were recently reported[74] at noise-free stations (far from industrialized regions) having long duration, i.e., of the order of several weeks. As we shall see, our results described in Sec. IV are in essential agreement with those obtained in the innovative and exhaustive study of Ma *et al.*[72] Before proceeding to our results, we will briefly summarize DFA and natural time analysis in Sec. II, and then present in Sec. III the most recent SES data along with their analysis in natural time. In Sec. V, we summarize our conclusions.

II. DETRENDED FLUCTUATION ANALYSIS AND NATURAL TIME

We first sum the original time-series x_i and determine the profile $y(i) \equiv \Sigma_{k=1}^{i}(x_k - \tilde{x})$, $i = 1, \ldots, N$, where $\tilde{x}$ is the average value of x_i. We then divide this profile of length N into $N/l (\equiv N_l)$ nonoverlapping fragments of l-observations. Next, we define the detrended process $y_{l,\nu}(m)$, in the νth fragment, as the difference between the original value of the profile and the local (linear) trend. We then calculate the mean variance of the detrended process,

$$F^2(l) = \frac{1}{N_l} \sum_{\nu=1}^{N_l} f^2(l, \nu), \tag{1}$$

where

$$f^2(l, \nu) = \frac{1}{l} \sum_{m=1}^{l} y_{l,\nu}^2(m). \tag{2}$$

If $F(l) \sim l^{\alpha}$, the slope of the log $F(l)$ versus log l plot leads to the value of the exponent $\alpha_{\mathrm{DFA}} \equiv \alpha$. (This scaling exponent is a self-similarity parameter that represents the long-range power-law correlations of the signal.) If $\alpha_{\mathrm{DFA}} = 0.5$, there is no correlation and the signal is uncorrelated (white noise); if $\alpha_{\mathrm{DFA}} < 0.5$, the signal is anticorrelated; if $\alpha_{\mathrm{DFA}} > 0.5$, the signal is correlated and specifically the case $\alpha_{\mathrm{DFA}} = 1.5$ corresponds to the Brownian motion (integrated white noise).

We now briefly explain the natural time χ. In a time-series comprising N events, the natural time $\chi_k = k/N$ serves as an index[75] for the occurrence of the kth event. The evolution of the pair (χ_k, Q_k) is studied,[45,46,75–80] where Q_k denotes a quantity proportional to the *energy* released in the kth event. For dichotomous signals, which is frequently the case of SES activities, the quantity Q_k can be replaced by the duration of the kth pulse. By defining $p_k = Q_k / \Sigma_{n=1}^{N} Q_n$, we

have found[75] that the variance of the natural time χ weighted by p_k,

$$\kappa_1 = \langle \chi^2 \rangle - \langle \chi \rangle^2, \tag{3}$$

where $\langle f(\chi) \rangle \equiv \Sigma_{k=1}^{N} p_k f(\chi_k)$, may be used[45,46] for the identification of SES activities. Namely, the following relation should hold:

$$\kappa_1 \approx 0.070. \tag{4}$$

The entropy S in the natural time domain is defined as[46]

$$S \equiv \langle \chi \ln \chi \rangle - \langle \chi \rangle \ln \langle \chi \rangle. \tag{5}$$

It exhibits[77] Lesche[81,82] (experimental) stability, and for SES activities (critical dynamics) it is smaller[46] than the value $S_u (= \ln 2/2 - 1/4 \approx 0.0966)$ of a "uniform" (u) distribution (as defined in Refs. 45, 46, and 76, e.g., when all p_k are equal or Q_k are positive independent and identically distributed random variables of finite variance). In this case, κ_1 and S are designated $\kappa_u (=1/12)$ and S_u, respectively. Thus, $S < S_u$. The same holds for the value of the entropy obtained[77,79] upon considering the time reversal $\hat{T}$ (the operator $\hat{T}$ is defined by $\hat{T} p_k = p_{N-k+1}$), which is labeled by S_-.

In summary, the SES activities, in contrast to the signals produced by man-made electrical sources, when analyzed in natural time (see Sec. I), exhibit *infinitely* ranged temporal correlations[46,75] and obey the conditions[79]

$$\kappa_1 \approx 0.07 \tag{6}$$

and

$$S, S_- < S_u. \tag{7}$$

III. THE EXPERIMENTAL DATA

In Fig. 1(a), we depict the SES activity recorded at Ioannina station (Northwestern Greece) on 18 April 1995. It preceded the 6.6 earthquake on 13 May 1995, which was the strongest one in Greece during the 25 year period 1983–2007. The DFA results on these data will be presented in Sec. IV. In addition, a recent SES activity in Greece is depicted in Figs. 1(b) and 1(c). This has been recorded at Lamia station located in Central Greece during the period 27–30 December 2009. For the details of the subsequent seismicity, see Refs. 83 and 84.

The two signals in Figs. 1(a) and 1(b) have been classified as SES activities after analyzing them in natural time. In particular, for the signal in Fig. 1(a), straightforward application of natural time analysis leads to the conclusion that the conditions (6) and (7) are satisfied (see Table I of Ref. 77). Further, the DFA analysis of the natural representation of this signal gives an exponent $\alpha_{\mathrm{DFA}} = 0.95(4) \approx 1$. (We also note that the classification of this signal as SES activity had been previously achieved by independent procedures discussed[85] in the Royal Society Meeting that was held during 11–12 May 1995 before[86] the occurrence of the 6.6 earthquake on 13 May 1995.) For the long duration signal of Fig. 1(b), the procedure explained in detail in Ref. 47 was followed.

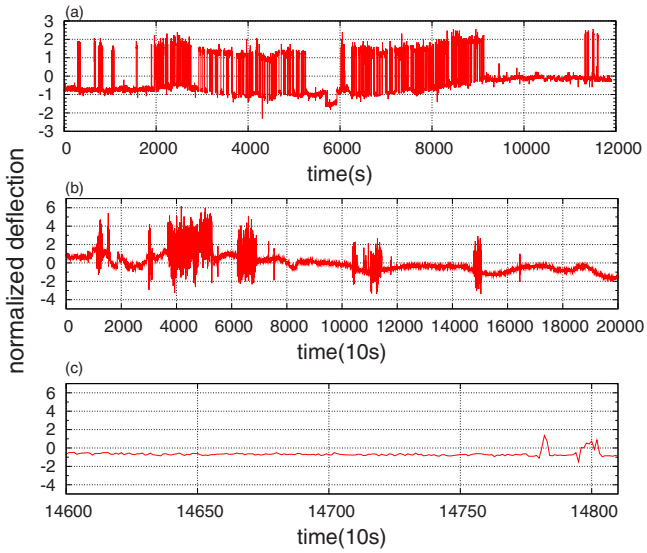

FIG. 1. (Color online) Examples of the electric field recordings in normalized units, i.e., by subtracting the mean value μ and dividing by the standard deviation σ. The following SES activities are depicted: (a) the one recorded on 18 April 1995 at Ioannina station; (b) the long duration SES activity recorded from 27 December 2010 to 30 December 2009 at Lamia station. (c) is an excerpt of (b) showing that, after long periods of quiescence, the electric field exhibits measurable excursions (transient pulses).

IV. DATA ANALYSIS AND RESULTS

Following Ma *et al.*,[72] we now describe the segmentation approach used here to generate surrogate signals $\tilde{u}(i)$ by randomly removing data segments of length L from the original signal $u(i)$. The percentage p of the data loss, i.e., the percentage of the data removed, characterizes the signal $\tilde{u}(i)$. The procedure followed is based on the construction of a binary time-series $g(i)$ of the same length as $u(i)$. The values of $u(i)$ that correspond to $g(i)$ equal to unity are kept, whereas the data of $u(i)$ when $g(i)$ equals zero are removed. The values of $u(i)$ kept are then concatenated to construct $\tilde{u}(i)$.

The binary time-series $g(i)$ is obtained as follows.[72] (i) We first generate the lengths $l_j = L$ with $j = 1, 2, \ldots, M$ of the removed segments by selecting M to be the smallest integer so that the total number of removed data satisfies the condition $\Sigma_{j=1}^{M} l_j \geq pN$. (ii) We then construct an auxiliary time-series $a(k)$ with $a(k) = L$ when $k = 1, 2, \ldots, M$ and $a(k) = 1$ when $k = M+1, \ldots, N-M(L+1)$ of size $N - M(L+1)$. (iii) We shuffle the time-series $a(k)$ randomly to obtain $\tilde{a}(k)$. (iv) We then append $\tilde{a}(k)$ to obtain $g(i)$: if $\tilde{a}(k) = 1$ we keep it, but we replace all $\tilde{a}(k) = L$ with L elements of value "0" and one element with value "1." In this way, a binary series $g(i)$ is obtained, which has a size equal to the one of the original signal $u(i)$. We then construct the surrogate signal $\tilde{u}(i)$ by simultaneously scanning the original signal $u(i)$ and the binary series $g(i)$, removing the ith element of $u(i)$ if $g(i) = 0$ and concatenating the segments of the remaining data to $\tilde{u}(i)$.

The resulting signal $\tilde{u}(i)$ is later analyzed in natural time, thus leading to the quantities κ_1, S, and S_- as well as to the DFA exponent α_{DFA} in natural time. Such an example is given in Fig. 2, which was drawn on the basis of the SES activity data depicted in Fig. 1(a).

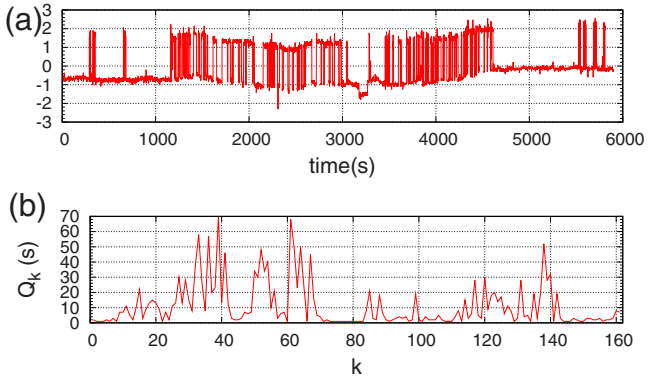

FIG. 2. (Color online) (a) Example of a surrogate time-series (in normalized units as in Fig. 1) obtained by removing segments of length $L=200$ from the signal of Fig. 1(a) with 50% data loss (i.e., $p=0.50$). (b) The natural time representation of (a). The values obtained from the analysis of (b) in natural time are $\kappa_1=0.067(4)$, $S=0.076(4)$, $S_-=0.071(4)$, and $\alpha_{\mathrm{DFA}}=0.90(5)$.

Typical DFA plots, obtained for $L=200$ and $p=30\%$, 50%, and 70%, are given in Fig. 3. For the sake of comparison, this figure also includes the case of no data loss (i.e., $p=0$). We notice a gradual decrease of α_{DFA} upon increasing the data loss, which affects our ability to recognize a signal as SES activity.

In order to evaluate our ability to identify SES activities from the natural time analysis of surrogate signals with various levels of data loss, three procedures have been attempted:

Procedure 1: Investigation whether α_{DFA}, which resulted from the DFA analysis of the natural time representation of a signal, belongs to the range $0.85 \leq \alpha_{\mathrm{DFA}} \leq 1.0$. If it does, the signal is then classified as SES activity. Figure 4(a) shows that for a given amount of data loss ($p=$const), upon increasing the length L of the randomly removed segment, the probability p_1 of achieving, after making 5000 attempts (for a given value of p and L), the identification of the signal as SES activity is found to gradually increase versus L at small scales and stabilizes at large scales. For example, when con-

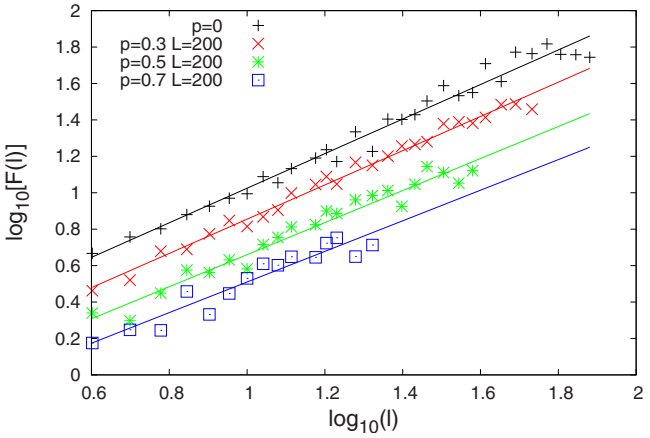

FIG. 3. (Color online) The dependence of the DFA measure $F(l)$ vs the scale l in natural time: we increase the percentage of data loss p by removing segments of length $L=200$ samples from the signal of Fig. 1(a). The black (plus) symbols correspond to no data loss ($p=0$), the red (crosses) to 30% data loss ($p=0.3$), the green (asterisks) to 50% data loss ($p=0.5$), and the blue (squares) to 70% data loss ($p=0.7$). Except for the case $p=0$, the data have been shifted vertically for the sake of clarity. The slopes of the corresponding straight lines that fit the data lead to $\alpha_{\mathrm{DFA}}=0.95$, 0.94, 0.88, and 0.84 from top to bottom, respectively. They correspond to the average values of α_{DFA} obtained from 5000 surrogate time-series that were generated with the method of surrogate by Ma *et al.* (Ref. 72) (see the text).

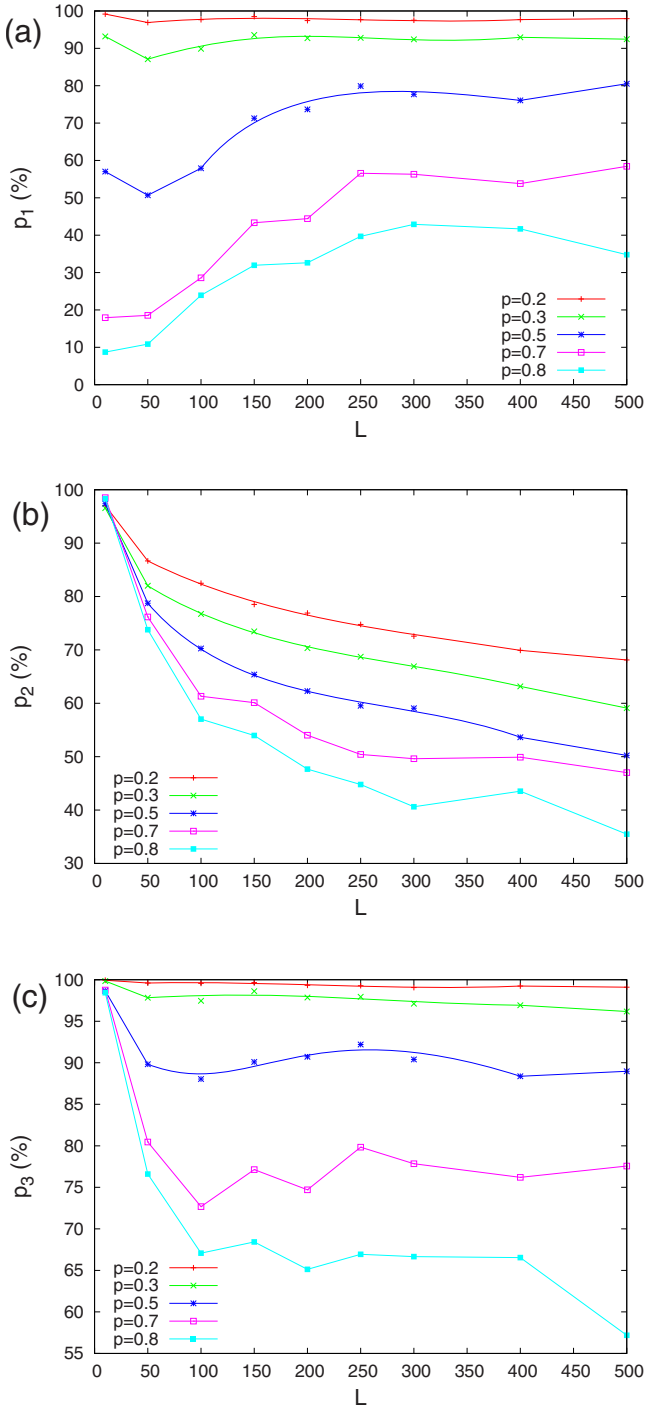

FIG. 4. (Color online) The probabilities (a) p_1, (b) p_2, and (c) p_3 to recognize the signal of Fig. 1(a) as true SES activity when considering various percentages of data loss $p=0.2$, 0.3, 0.5, 0.7, and 0.8 as a function of the length L of the contiguous samples removed. The removal of large segments leads to better results when using DFA in natural time (a), whereas the opposite holds when using the conditions of Eqs. (6) and (7) for κ_1, S, and S_- (b). The optimum selection (c) for the identification of a signal as SES activity consists of a proper combination of the aforementioned procedures in (a) and (b), see the text. The values presented have been obtained from 5000 surrogate time-series (for a given value of p and L), and hence they have a plausible error of 1.4% ($\approx 1/\sqrt{5000}$).

sidering the case of 70% data loss [open squares in Fig. 4(a)] the probability p_1 is close to 20% for $L=50$; it increases to $p_1 \approx 30\%$ for $L=100$ and finally stabilizes around 50% for lengths $L=300-500$. This is essentially consistent with the earlier findings of Ma *et al.*[72] who noticed that removing the same percentage of data using longer (and fewer) segments has a lesser impact on the scaling behavior compared to removing segments with a smaller average length.

Procedure 2: Investigation whether the quantities κ_1, S, and S_- (which resulted from the analysis of a signal in natural time) obey the conditions (6) and (7), i.e., $|\kappa_1 - 0.070| \leq 0.01$ and $S, S_- < 0.0966$. If they do so, the signal is classified as SES activity. Figure 4(b) shows that for a given amount of data loss, the probability p_2 of achieving the signal identification as SES activity—that results after making 5000 attempts for each L value—gradually decreases when moving from small to large scales. Note that for the smallest length scale investigated, i.e., $L=10$ (which is more or less comparable—if we consider the sampling frequency of 1 sample/s—with the average duration of ≈ 11 s of the transient pulses that constitute the signal), the probability p_2 reaches values close to 100% even for the extreme data loss of 80%. This is understood in the context that the quantities κ_1, S, and S_- remain almost unaffected when randomly removing segments with lengths comparable to the average pulse's duration. This is consistent with our earlier finding[77] that the quantities κ_1, S, and S_- are experimentally stable (Lesche's stability), meaning that they exhibit only slight variations when deleting (due to experimental errors) a small number of pulses. On the other hand, at large scales of L, p_2 markedly decreases. This may be understood if we consider that, at such scales, each segment of contiguous L samples removed comprises on the average a considerable number of pulses the removal of which may seriously affect the quantities κ_1, S, and S_-. As an example, for 80% data loss [solid squares in Fig. 4(b)], and for lengths $L=400-500$, the probability p_2 of identifying a true SES activity is around 40%.

Interestingly, a closer inspection of Figs. 4(a) and 4(b) reveals that p_1 and p_2 play complementary roles. In particular, at small scales of L, p_1 increases but p_2 decreases versus L. At large scales, where p_1 reaches (for considerable values of data loss) its largest value, the p_2 value becomes small. Inspired from this complementary behavior of p_1 and p_2, we proceeded to the investigation of a combined procedure:

Procedure 3: In this procedure, a signal is identified as SES activity when *either* the condition $0.85 \leq \alpha_{\mathrm{DFA}} \leq 1.0$ *or* the relations (6) and (7) are satisfied. The probability p_3 of achieving such an identification, after making 5000 attempts (for a given value of p and L), is plotted in Fig. 4(c). The results are remarkable since, even at significant values of data loss, e.g., $p=70\%$ or 80%, the probability p_3 of identifying a SES activity at scales $L=100-400$ remains relatively high, i.e., $p_3 \approx 75\%$ and 65%, respectively (cf. note also that the value of p_3 reaches values close to 100% at small scales $L=10$). This is important from practical point of view, because it states, for example, the following: even if the records of a station are contaminated by considerable noise, say 70% of the time of its operation, the remaining 30% of the noncontaminated segments have a chance of $\sim 75\%$ to correctly identify a SES activity. The chances increase considerably, i.e., to $p_3 \approx 90\%$, if only half of the recordings are noisy.

The aforementioned results have been deduced from the analysis of a SES activity lasting around 3 h. In cases of SES activities with appreciably longer duration, e.g., a few to several days[47,87] detected in Greece or a few months in Japan,[74] the results should become appreciably better.

V. CONCLUSIONS

We start our conclusions by recalling that the distinction between SES activities (critical dynamics, infinitely ranged temporal correlations) and artificial (man-made) noise remains an extremely difficult task, even without any data loss, when solely focusing on the original time-series of electrical records which are, of course, in conventional time. On the other hand, when combining natural time with DFA analysis, such a distinction becomes possible even after significant data loss. In particular we showed for example that even when randomly removing 50% of the data, we have a probability (p_3) around 90%, or larger, to identify correctly a SES activity. This probability becomes somewhat smaller, i.e., 75%, when the data loss increases to 70%. To achieve this goal, the proper procedure is the following: the signal is first represented in natural time and then analyzed in order to deduce the quantities κ_1, S, and S_- as well as the exponent α_{DFA} from the slope of the log-log plot of the DFA analysis in natural time. We then examine whether the latter slope has a value close to unity or the conditions $\kappa_1 \approx 0.070$ and S, $S_- < S_u$ are obeyed. In other words, the consequences caused by an undesirable severe data loss can be markedly reduced upon taking advantage of the DFA and natural time analysis.

[1] J. B. Bassingthwaighte, L. Liebovitch, and B. J. West, *Fractal Physiology* (Oxford University Press, Oxford, UK, 1994).
[2] M. M. Malik and A. Camm, *Heart Rate Variability* (Futura, Armonk, NY, 1995).
[3] H. E. Stanley, Nature (London) **378**, 554 (1995).
[4] H. E. Hurst, Trans. Am. Soc. Civ. Eng. **116**, 770 (1951).
[5] B. B. Mandelbrot and J. R. Wallis, Water Resour. Res. **5**, 321 (1969).
[6] R. L. Stratonovich, *Topics in the Theory of Random Noise* (Gordon and Breach, New York, 1981), Vol. I.
[7] C.-K. Peng, S. V. Buldyrev, S. Havlin, M. Simons, H. E. Stanley, and A. L. Goldberger, Phys. Rev. E **49**, 1685 (1994).
[8] M. S. Taqqu, V. Teverovsky, and W. Willinger, Fractals **3**, 785 (1995).
[9] C.-K. Peng, S. V. Buldyrev, A. L. Goldberger, S. Havlin, M. Simons, and H. E. Stanley, Phys. Rev. E **47**, 3730 (1993).
[10] R. N. Mantegna, S. V. Buldyrev, A. L. Goldberger, S. Havlin, C. K. Peng, M. Simons, and H. E. Stanley, Phys. Rev. Lett. **73**, 3169 (1994).
[11] S. Havlin, S. V. Buldyrev, A. L. Goldberger, R. N. Mantegna, S. M. Ossadnik, C. K. Peng, M. Simon, and H. E. Stanley, Chaos, Solitons Fractals **6**, 171 (1995).
[12] C. K. Peng, S. V. Buldyrev, A. L. Goldberger, S. Havlin, R. N. Mantegna, M. Simon, and H. E. Stanley, Physica A **221**, 180 (1995).
[13] S. Havlin, S. V. Buldyrev, A. L. Goldberger, R. N. Mantegna, C. K. Peng, M. Simon, and H. E. Stanley, Fractals **3**, 269 (1995).
[14] R. N. Mantegna, S. V. Buldyrev, A. L. Goldberger, S. Havlin, C.-K. Peng, M. Simons, and H. E. Stanley, Phys. Rev. Lett. **76**, 1979 (1996).
[15] S. V. Buldyrev, N. V. Dokholyan, A. L. Goldberger, S. Havlin, C. K. Peng, H. E. Stanley, and G. M. Viswanathan, Physica A **249**, 430 (1998).
[16] H. E. Stanley, S. V. Buldyrev, A. L. Goldberger, S. Havlin, C. K. Peng, and M. Simon, Physica A **273**, 1 (1999).
[17] C. K. Peng, S. Havlin, and H. E. Stanley, Chaos **5**, 82 (1995).
[18] K. K. L. Ho, G. B. Moody, C.-K. Peng, J. E. Mietus, M. G. Larson, D. Levy, and A. L. Goldberger, Circulation **96**, 842 (1997).
[19] P. Ch. Ivanov, A. Bunde, L. A. N. Amaral, S. Havlin, J. Fritsch-Yelle, R. M. Baevsky, H. E. Stanley, and A. L. Goldberger, EPL **48**, 594 (1999).

[20]Y. Ashkenazy, P. Ch. Ivanov, S. Havlin, C. K. Peng, Y. Yamamoto, A. L. Goldberger, and H. E. Stanley, Comput. Cardiol. **27**, 139 (2000).
[21]Y. Ashkenazy, P. Ch. Ivanov, S. Havlin, C.-K. Peng, A. L. Goldberger, and H. E. Stanley, Phys. Rev. Lett. **86**, 1900 (2001).
[22]P. Ch. Ivanov, L. A. N. Amaral, A. L. Goldberger, S. Halvin, M. G. Rosenblum, H. E. Stanley, and Z. R. Struzik, Chaos **11**, 641 (2001).
[23]J. W. Kantelhardt, Y. Ashkenazy, P. Ch. Ivanov, A. Bunde, S. Havlin, T. Penzel, J.-H. Peter, and H. E. Stanley, Phys. Rev. E **65**, 051908 (2002).
[24]R. Karasik, N. Sapir, Y. Ashkenazy, P. Ch. Ivanov, I. Dvir, P. Lavie, and S. Havlin, Phys. Rev. E **66**, 062902 (2002).
[25]P. Ch. Ivanov, Z. Chen, K. Hu, and H. E. Stanley, Physica A **344**, 685 (2004).
[26]D. T. Schmitt and P. Ch. Ivanov, Am. J. Physiol. Regulatory Integrative Comp. Physiol. **293**, R1923 (2007).
[27]D. T. Schmitt, P. K. Stein, and P. Ch. Ivanov, IEEE Trans. Biomed. Eng. **56**, 1564 (2009).
[28]K. Hu, P. Ch. Ivanov, Z. Chen, M. F. Hilton, H. E. Stanley, and S. A. Shea, Physica A **337**, 307 (2004).
[29]P. Ch. Ivanov, K. Hu, M. F. Hilton, S. A. Shea, and H. E. Stanley, Proc. Natl. Acad. Sci. U.S.A. **104**, 20702 (2007).
[30]P. Ch. Ivanov, IEEE Eng. Med. Biol. Mag. **26**, 33 (2007).
[31]K. Hu, F. A. J. L. Scheer, P. Ch. Ivanov, R. M. Buijs, and S. A. Shea, Neuroscience **149**, 508 (2007).
[32]K. Ivanova and M. Ausloos, Physica A **274**, 349 (1999).
[33]E. Koscielny-Bunde, A. Bunde, S. Havlin, H. E. Roman, Y. Goldreich, and H.-J. Schellnhuber, Phys. Rev. Lett. **81**, 729 (1998).
[34]P. Talkner and R. O. Weber, Phys. Rev. E **62**, 150 (2000).
[35]A. Bunde, S. Havlin, E. Koscielny-Bunde, and H. J. Schellnhuber, Physica A **302**, 255 (2001).
[36]R. A. Monetti, S. Havlin, and A. Bunde, Physica A **320**, 581 (2003).
[37]A. Bunde, J. F. Eichner, J. W. Kantelhardt, and S. Havlin, Phys. Rev. Lett. **94**, 048701 (2005).
[38]Y. H. Liu, P. Cizeau, M. Meyer, C. K. Peng, and H. E. Stanley, Physica A **245**, 437 (1997).
[39]N. Vandewalle and M. Ausloos, Physica A **246**, 454 (1997).
[40]N. Vandewalle and M. Ausloos, Phys. Rev. E **58**, 6832 (1998).
[41]M. Ausloos, N. Vandewalle, P. Boveroux, A. Minguet, and K. Ivanova, Physica A **274**, 229 (1999).
[42]N. Vandewalle, M. Ausloos, and P. Boveroux, Physica A **269**, 170 (1999).
[43]M. Ausloos, Physica A **285**, 48 (2000).
[44]M. Ausloos and K. Ivanova, Phys. Rev. E **63**, 047201 (2001).
[45]P. A. Varotsos, N. V. Sarlis, and E. S. Skordas, Phys. Rev. E **67**, 021109 (2003).
[46]P. A. Varotsos, N. V. Sarlis, and E. S. Skordas, Phys. Rev. E **68**, 031106 (2003).
[47]P. A. Varotsos, N. V. Sarlis, and E. S. Skordas, Chaos **19**, 023114 (2009).
[48]P. Varotsos and K. Alexopoulos, Tectonophysics **110**, 73 (1984).
[49]P. Varotsos and K. Alexopoulos, Tectonophysics **110**, 99 (1984).
[50]P. Varotsos, K. Alexopoulos, K. Nomicos, and M. Lazaridou, Nature (London) **322**, 120 (1986).
[51]P. Varotsos, K. Alexopoulos, K. Nomicos, and M. Lazaridou, Tectonophysics **152**, 193 (1988).
[52]P. Varotsos and M. Lazaridou, Tectonophysics **188**, 321 (1991).
[53]P. Varotsos, K. Alexopoulos, and M. Lazaridou, Tectonophysics **224**, 1 (1993).
[54]P. Varotsos, K. Eftaxias, M. Lazaridou, G. Antonopoulos, J. Makris, and J. Poliyiannakis, Geophys. Res. Lett. **23**, 1449, doi:10.1029/96GL01437 (1996).
[55]P. Varotsos, N. Sarlis, and E. Skordas, Proc. Jpn. Acad., Ser. B: Phys. Biol. Sci. **77**, 87 (2001).
[56]P. Varotsos, N. Sarlis, and E. Skordas, Proc. Jpn. Acad., Ser. B: Phys. Biol. Sci. **77**, 93 (2001).
[57]N. Sarlis and P. Varotsos, J. Geodyn. **33**, 463 (2002).
[58]P. A. Varotsos, N. V. Sarlis, and E. S. Skordas, Phys. Rev. Lett. **91**, 148501 (2003).
[59]P. Ch. Ivanov, L. A. N. Amaral, A. L. Goldberger, S. Havlin, M. G. Rosenblum, Z. Struzik, and H. E. Stanley, Nature (London) **399**, 461 (1999).
[60]R. O. Weber and P. Talkner, J. Geophys. Res., [Atmos.] **106**, 20131, doi:10.1029/2001JD000548 (2001).
[61]J. Kantelhardt, S. A. Zschiegner, E. Koscienly-Bunde, A. Bunde, S. Havlin, and H. E. Stanley, Physica A **316**, 87 (2002).
[62]J. F. Muzy, E. Bacry, and A. Arneodo, Int. J. Bifurcation Chaos Appl. Sci. Eng. **4**, 245 (1994).
[63]P. Varotsos and K. Alexopoulos, *Thermodynamics of Point Defects and Their Relation with Bulk Properties* (North-Holland, Amsterdam, 1986).
[64]P. Varotsos, *The Physics of Seismic Electric Signals* (TERRAPUB, Tokyo, 2005).
[65]P. Varotsos, Phys. Rev. B **13**, 938 (1976).
[66]P. Varotsos and K. Alexopoulos, J. Phys. Chem. Solids **39**, 759 (1978).
[67]P. Varotsos, W. Ludwig, and K. Alexopoulos, Phys. Rev. B **18**, 2683 (1978).
[68]P. Varotsos and K. Alexopoulos, J. Phys. C **12**, L761 (1979).
[69]P. Varotsos and K. Alexopoulos, Phys. Rev. B **30**, 7305 (1984).
[70]P. Varotsos, J. Appl. Phys. **101**, 123503 (2007).
[71]M. Ausloos and R. Lambiotte, Phys. Rev. E **73**, 011105 (2006).
[72]Q. D. Y. Ma, R. P. Bartsch, P. Bernaola-Galván, M. Yoneyama, and P. Ch. Ivanov, Phys. Rev. E **81**, 031101 (2010).
[73]Y. Orihara, M. Kamogawa, T. Nagao, and S. Uyeda, Proc. Jpn. Acad., Ser. B: Phys. Biol. Sci. **85**, 435 (2009).
[74]S. Uyeda, M. Kamogawa, and H. Tanaka, J. Geophys. Res., [Solid Earth] **114**, B02310, doi:10.1029/2007JB005332 (2009).
[75]P. A. Varotsos, N. V. Sarlis, and E. S. Skordas, Phys. Rev. E **66**, 011902 (2002).
[76]P. A. Varotsos, N. V. Sarlis, E. S. Skordas, and M. S. Lazaridou, Phys. Rev. E **70**, 011106 (2004).
[77]P. A. Varotsos, N. V. Sarlis, H. K. Tanaka, and E. S. Skordas, Phys. Rev. E **71**, 032102 (2005).
[78]P. A. Varotsos, N. V. Sarlis, E. S. Skordas, and M. S. Lazaridou, Phys. Rev. E **71**, 011110 (2005).
[79]P. A. Varotsos, N. V. Sarlis, E. S. Skordas, H. K. Tanaka, and M. S. Lazaridou, Phys. Rev. E **73**, 031114 (2006).
[80]P. A. Varotsos, N. V. Sarlis, E. S. Skordas, H. K. Tanaka, and M. S. Lazaridou, Phys. Rev. E **74**, 021123 (2006).
[81]B. Lesche, J. Stat. Phys. **27**, 419 (1982).
[82]B. Lesche, Phys. Rev. E **70**, 017102 (2004).
[83]P. A. Varotsos, N. V. Sarlis, and E. S. Skordas, "Detrended fluctuation analysis of the magnetic and electric field variations that precede rupture," e-print arXiv:0904.2465v10.
[84]The SES activity of Fig. 1(b) originated the natural time analysis of the seismicity in the area N(38.0–39.0) E(21.5–23.7) after 27 December 2009, described in the previous reference. This type of analysis revealed that on the day (6 March 2010) of submission of the present paper, the critical point has been approached and an impending mainshock was imminent. Actually, a few days later, i.e., on 9 March 2010, at 2:55 UT a magnitude (Ms(ATH)=)5.6 earthquake occurred with an epicenter at 38.87N 23.65E; see E. S. Skordas, N. V. Sarlis, and P. A. Varotsos, "Effect of significant data loss on identifying electric signals that precede rupture by detrended fluctuation analysis in natural time," e-print arXiv:1003.1383v1.
[85]P. Varotsos, M. Lazaridou, K. Eftaxias, G. Antonopoulos, J. Makris, and J. Kopanas, in *The Critical Review of VAN: Earthquake Prediction from Seismic Electric Signals*, edited by S. J. Lighthill (World Scientific, Singapore, 1996), pp. 29–76.
[86]J. Lighthill, in *The Critical Review of VAN: Earthquake Prediction from Seismic Electric Signals*, edited by S. J. Lighthill (World Scientific, Singapore, 1996), pp. 373–376.
[87]N. V. Sarlis, E. S. Skordas, M. S. Lazaridou, and P. A. Varotsos, Proc. Jpn. Acad., Ser. B: Phys. Biol. Sci. **84**, 331 (2008).